Journal of Thermal Analysis and Calorimetry, Vol. 80 (2005) 663–670

SYNTHESIS OF LEAD MAGNESIUM NIOBATE AND La-MODIFIED LEAD MAGNESIUM NIOBATE USING DIFFERENT Mg PRECURSORS

A. Ianculescu[1*], *A. Brăileanu*[2], *I. Pasuk*[3] *and C. Popescu*[4]

[1]University 'Politehnica' of Bucharest, 1 Gh. Polizu, P.O. Box 12-134, Bucharest, Romania
[2]Institute of Physical Chemistry, 202 Spl. Independenţei, Bucharest, Romania
[3]SC ICPE SA, 313 Spl. Unirii, Bucharest, Romania
[4]The German Wool Research Institute an der RWTH Aachen, Veltmanplatz 8, Aachen, Germany

In the present study, the effect of the partial replacement of Pb^{2+} by La^{3+} in the lead magnesium niobate $Pb(Mg_{1/3}Nb_{2/3})O_3$ (PMN) perovskite structure was examined, taking into account the Mg-source. Pure lead magnesium niobate (PMN) and lanthanum-modified lead magnesium niobate (PLMN) having composition $(Pb_{1-x}La_x)(Mg_{1+x/3}Nb_{2-x/3})O_3$ with x=0.2 were elaborated.

The phase formation was investigated by DTA/TG methods correlated with X-ray diffraction, performed on materials obtained in non-isothermal conditions. The diffraction data for the ceramics obtained by isothermal treatments emphasized the influence of the lanthanum on the crystal structure, inducing the doubling of the unit cell parameter. SEM investigations pointed out the lanthanum inhibitor effect on the grain growth process, leading to a uniform grain distribution.

Keywords: *columbite, perovskite, PLMN, PMN, pyrochlore*

Introduction

Among the lead-based relaxor ferroelectric materials of general formula $Pb(B'B'')O_3$, lead magnesium niobate, $Pb(Mg_{1/3}Nb_{2/3})O_3$ (PMN) is probably the most widely studied one because of its excellent dielectric and electrostrictive properties. However, a significant problem concerning PMN ceramics is the difficulty in preparing a single-phase material of only perovskite structure without the appearance of a pyrochlore phase that can be detrimental to the dielectric properties [1–3]. Various synthesis techniques for suppressing the formation of pyrochlore-type compound (i.e. columbite method [4–6] and mechanical activated synthesis [7–9]) have been reported in the literature.

Former studies [10, 11] showed that the degree of ordering and the size of ordered domains can be enhanced by incorporating lanthanum into lead magnesium niobate lattice.

Although the formation mechanism of PMN was studied [12–14], it remains however a very controversial process probably because of the different synthesis conditions and precursors used in these reports. On the other hand, unlike other substituted perovskites [15–18], for the phase formation mechanism of lanthanum-modified lead magnesium niobate no data were reported, even its structural characteristics were widely examined [19–23].

The present work is dedicated to the study of the formation mechanism of PMN, as well as of La-modified PMN obtained via columbite route, taking into account the magnesium source. The influence of the magnesium precursor on the PMN and PLMN ceramics microstructure was also investigated. Correlations between phase composition, processing factors and properties (crystalline structure and microstructure) were established.

Experimental

The starting materials were reagent-grade PbO (Fluka), La_2O_3 (Loba Feinchemie), MgO (Merck) $(MgCO_3)_4 \cdot Mg(OH)_2 \cdot 5H_2O$ (Carlo Erba) and Nb_2O_5 (Johnson Matthey Chemicals Ltd.) powders.

The samples prepared for this study, using two Mg-precursors were stoichiometric columbite (MN1a, MN2a) and pure lead magnesium niobate (PMN1 and PMN2), as well as non-stoichiometric columbite (MN1b, MN2b) and La-modified lead magnesium niobate (PLMN1, PLMN2).

The perovskite phases composition was expressed by the formula $(Pb_{1-x}La_x)(Mg_{(1+x)/3}Nb_{(2-x)/3})O_3$, where x=0; 0.2. The non-stoichiometric columbite was prepared in order to increase the Mg/Nb ratio, which balances the donor charge of La^{3+} and prevents the formation of A-site vacancies in the perovskite lattice of PLMN solid solutions. The composition of these samples is presented in Table 1.

* Author for correspondence: a.ianculescu@rdslink.ro

1388–6150/$20.00

Akadémiai Kiadó, Budapest, Hungary
Springer, Dordrecht, The Netherlands

Table 1 The studied compositions

Symbol	Composition	Mg-precursor
MN1a	$MgNb_2O_6$	MgO
MN1b	$Mg_{1.2}Nb_{1.8}O_{5.7}$	MgO
MN2a	$MgNb_2O_6$	$(MgCO_3)_4{\cdot}Mg(OH)_2{\cdot}5H_2O$
MN2b	$Mg_{1.2}Nb_{1.8}O_{5.7}$	$(MgCO_3)_4{\cdot}Mg(OH)_2{\cdot}5H_2O$
PMN1	$Pb(Mg_{0.33}Nb_{0.66})O_3$	MgO
PMN2	$Pb(Mg_{0.33}Nb_{0.66})O_3$	$(MgCO_3)_4{\cdot}Mg(OH)_2{\cdot}5H_2O$
PLMN1	$Pb_{0.8}La_{0.2}(Mg_{0.4}Nb_{0.6})O_3$	MgO
PLMN2	$Pb_{0.8}La_{0.2}(Mg_{0.4}Nb_{0.6})O_3$	$(MgCO_3)_4{\cdot}Mg(OH)_2{\cdot}5H_2O$

Synthesis of PMN and La-modified PMN samples was carried out by a two-stage process, the columbite method, proposed by Swartz and Shrout [4].

For the PMN mixtures, in the first stage, MgO and Nb_2O_5 powders were prereacted at 1000°C in air to form columbite:

$$MgO+Nb_2O_5 \rightarrow MgNb_2O_6 \quad (1)$$

In the second stage, the prefabricated $MgNb_2O_6$ was reacted with appropriate amounts of PbO at 870°C to form the PMN perovskite structure:

$$MgNb_2O_6+3PbO \rightarrow Pb_3(MgNb_2)O_9 \text{ (PMN)} \quad (2)$$

For the PLMN mixtures, the first step implies the formation of non-stoichiometric columbite, according to reaction (3):

$$(1+x)MgO+(2-x)1/2Nb_2O_5 \rightarrow Mg_{1+x}Nb_{2-x}O_{6-3x/2} \quad (3)$$

Taking into account the fact that in our case x=0.2, the reaction (3) can be expressed as follows:

$$1.2MgO+1.8{\cdot}1/2Nb_2O_5 \rightarrow Mg_{1.2}Nb_{1.8}O_{5.7} \quad (3')$$

To form La-modified lead magnesium niobate, PbO and La_2O_3 were added to the non-stoichiometric columbite, according to reaction (4)

$$Mg_{1+x}Nb_{2-x}O_{6-3x/2}+3(1-x)PbO+3x/2La_2O_3 \rightarrow \rightarrow Pb_{3(1-x)}La_{3x}(Mg_{1+x}Nb_{2-x})O_9 \quad (4)$$

particularly,

$$Mg_{1.2}Nb_{1.8}O_{5.7}+2.4PbO+0.3La_2O_3 \rightarrow \rightarrow 3Pb_{0.8}La_{0.2}(Mg_{0.4}Nb_{0.6})O_3 \quad (4')$$

Since the hygroscopic MgO is carbonated and hydrated during the storing, a prior annealing was carried out up to 1000°C in order to calculate the calcination loss and to have a suitable 'active' MgO amount for a stoichiometric reaction with Nb_2O_5.

After Nb_2O_5 and $MgO/(MgCO_3)_4{\cdot}Mg(OH)_2{\cdot}5H_2O$ ball-milling (for 10 h) in isopropanol and subsequent drying, the mixture was heated in air with 5 K min^{-1} up to 1000ºC with 6 h plateau. The product (MN) was then ball-milled in alcohol again for 10 h with appropriate amounts of PbO and La_2O_3 and annealed in air, with the same heating rate at 870ºC for 6 h. The calcined powders with polyvinyl alcohol (PVA) added as binder, were pressed into pellets of 10 mm diameter and ~3 mm thickness, which were then sintered for 4 h in air at 870 and 1200ºC, respectively. Sintering was performed inside closed platinum crucibles and the pellets were covered with powders of the same composition to minimize the lead loss during the thermal treatments.

In order to evidence the changes occurring during the heating process, DTA and TG investigations of raw materials, as well as of the mixtures mentioned were performed. The thermal behaviour was studied by simultaneous TG/DTA measurements up to 1000ºC in static air atmosphere, with heating rates of 10 and 2.5 K min^{-1}, using Pt crucibles, with a Derivatograph supplied by MOM Hungary, system Paulik–Paulik–Erdey, type OD 103.

The phase composition and the structural parameters of the samples were studied by X-ray diffraction (XRD) with a Brucker-AXS D8 diffractometer, using Ni-filtered CuK_α radiation. X-ray diffraction analyses were carried out both on samples resulting from non-isothermal treatments up to different temperatures and on samples resulting from isothermal treatments. The lattice unit cell parameters have been determined by the least squares method, based on the position of nine or ten well defined diffraction lines. The program takes into account the gain in precision with increasing diffraction angles. The uncertainty of the diffraction angle (2θ) measurement for powder samples is evaluated to be around 0.04°, so that we have estimated that the uncertainty of the calculated parameter is not more than 0.001 Å. We consider that there is no systematic measurement error of the diffraction angle due to the good alignment of the goniometer.

The microstructural features of the samples were investigated by scanning electron microscopy (SEM) using a JEOL JSM-6400. The sinterability of PMN and PLMN ceramics was estimated by means of the values of relative density calculated as ratio between the apparent density determined by the hydrostatic method and the theoretical density.

Results and discussion

Columbite formation and characterization

DTA curves of the initial mixtures of Nb_2O_5 and Mg-precursors, corresponding to the MN1a and MN2a compositions are presented in Fig. 1. Similar behaviour was noticed also for MN1b and MN2b compositions.

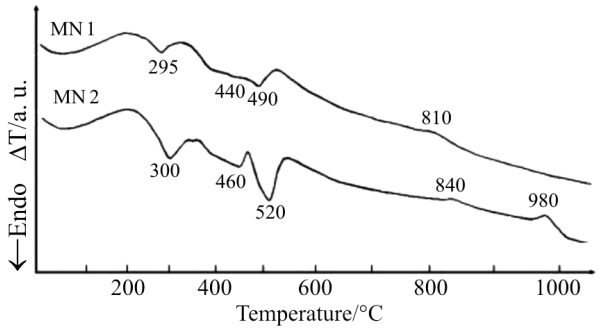

Fig. 1 DTA curves of the stoichiometric columbite compositions

Both DTA curves show low temperature endothermic effects corresponding to the volatiles release: water of crystallization (~300°C), hydroxyl water (440 and 460°C, respectively) and CO_2 (490 and 520°C, respectively) [24] and also a high temperature broad peak situated at 810°C for MN1a and 840°C for MN2a. This effect is probably due to the columbite ($MgNb_2O_6$) formation. A supplementary exothermic effect at 980°C is noticed only on the second (MN2a) curve, which can be assigned to a secondary $Mg_4Nb_2O_9$ compound formation. These results are in agreement with the X-ray diffraction data of the columbite samples (obtained after isothermal treatment at 1000°C/6 h), which pointed out the presence of the $Mg_4Nb_2O_9$ (JCPDS 38-1459) as a secondary phase, beside the $MgNb_2O_6$ (JCPDS 25-0526) major phase, especially for the MN2a composition (Fig. 2).

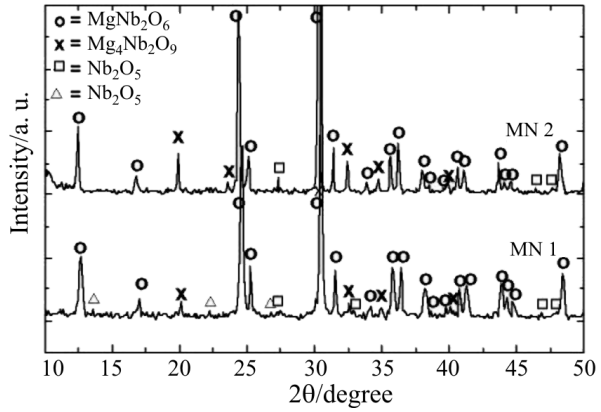

Fig. 2 XRD patterns of the stoichiometric columbite compositions

In the case of MN1a composition this secondary phase was hardly identified at the Roentgen detection limit, even in these isothermal conditions, which could explain the lack of corresponding effect on the DTA curve of MN1a composition. Therefore, we can conclude that the Mg carbonate precursor induces the enhancing of the $Mg_4Nb_2O_9$ secondary phase, comparing to MgO precursor.

As a consequence of the $Mg_4Nb_2O_9$ formation, small amounts of unreacted Nb_2O_5 were also identified.

PMN and PLMN formation and characterization

Thermal analysis

The thermal behaviour of the mixtures ($MgNb_2O_6$ +PbO) corresponding to PMN1 and PMN2 are quite similar. Similar thermal analysis curves were noticed also for mixtures ($MgNb_2O_6$+PbO+La_2O_3) corresponding to PLMN1 and PLMN2. For this reason, only the DTA/TG curves of PMN2 and PLMN2 mixtures are presented in Figs 3a and b.

Below 400°C two endothermic effects (~250 and 340°C) due to the volatiles elimination (water from $La(OH)_3$ dehydration and organic residuals originated from solvent) are noticed [7]. For the PLMN2 mixture the second effect appears as a shoulder, as a consequence of the overlapping with another endothermic effect (380°C) assigned to the La precursor dehydration process. Indeed, the TG curve of the PLMN2 mixture

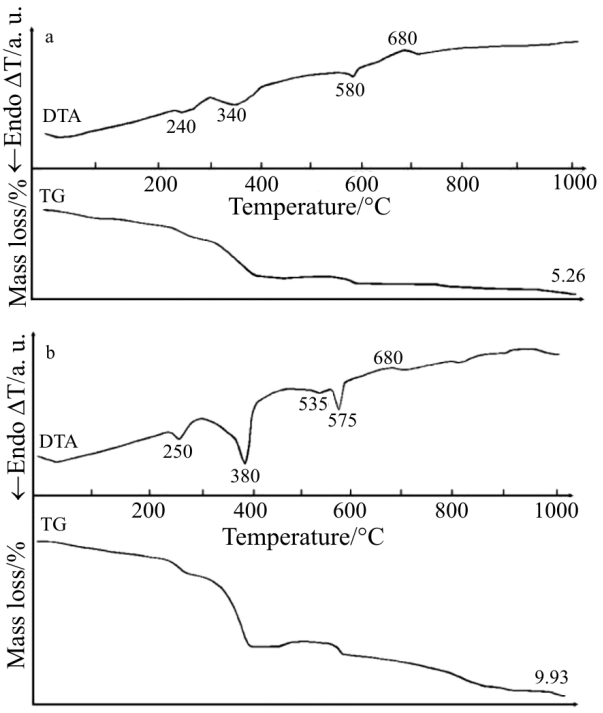

Fig. 3 DTA/TG curves of: a – PMN2 composition; b – PLMN2 composition

shows a more significant mass loss than that one specific to the PMN2 mixture. Because of the well-known tendency of La_2O_3 to take up moisture and CO_2 from atmosphere a supplementary small endothermic effect specific to the $La_2O_2CO_3$ decomposition is also remarked at ~535°C on the DTA curve of PLMN2 mixture. Over 400°C both compositions show the oxidation of PbO to Pb_3O_4 (more pronounced for PLMN2 as one can see on the TG curve), as well as the reduction of Pb_3O_4 to PbO (the endothermic peak at ~575°C). The broad exothermic effect situated at ~680ºC, emphasized for the both compositions, is probably determined by the perovskite skeleton formation.

The slow and continuous mass loss over 800°C, more pronounced for the PLMN2 mixture, is probably due to the PbO volatilization.

X-ray diffraction

X-ray diffraction patterns for the mixtures PMN1 and PMN2 non-isothermally treated up to 500°C pointed out only the presence of the reactants (columbite, PbO and traces of $Mg_4Nb_2O_9$), better crystallized for PMN1 (Figs 4a and b).

At 700°C the influence of the Mg-source is more visible. Thus, for the MgO precursor (PMN1 sample), almost a single phase composition consisting of the well-crystallized PMN perovskite (JCPDS 81-861) was obtained, whereas for the Mg carbonate precursor (PMN2 sample), at the same temperature, a small amount of $Pb_{1.83}(Mg_{0.29}Nb_{1.71})O_{6.39}$ minor pyrochlore phase (JCPDS 33-769) was detected. The very weak diffraction peak situated at 2θ=28.4° shows the presence of another $Pb_2Nb_2O_7$ (PN) pyrochlore phase identified at the detection limit (JCPDS 30-711). These residual pyrochlore phases are due to the reaction between 'free Nb_2O_5' in the columbite precursor and PbO. The higher the $Mg_4Nb_2O_5$ proportion in the columbite precursor, the higher the extra Nb_2O_5 amount and the higher the pyrochlore quantity in the PMN composition. This shows that an additional MgO amount, more significant in the case of using of magnesium carbonate precursor, is required to convert the extra Nb_2O_5 and $Mg_4Nb_2O_9$ to $MgNb_2O_6$, in order to obtain a pyrochlore-free PMN [13]. A reaction between PbO and $Mg_4Nb_2O_9$ to form PMN (Eq. (3)) could also takes place between 500–700°C, but taking into account the very small amount of $Mg_4Nb_2O_9$ identified at 500°C, no MgO product was detected at 700°C.

$$3PbO+Mg_4Nb_2O_9 \rightarrow Pb_3(MgNb_2)O_9+3MgO \quad (5)$$

Since only one high temperature exothermic effect (~680°C) was noticed on the DTA curve of PMN2, it seems probably that the perovskite and pyrochlore formation occurs simultaneously. This assumption is in agreement with the reaction sequence proposed by Sreedhar *et al*. [25], contrarily with Kim *et al*. work [26], which claims the formation of the pyrochlore phase after the perovskite one. Thus, it is obvious that the using of MgO precursor induces a columbite composition with a higher $MgNb_2O_6$ proportion (MN1a), which leads to a quantitative reaction with PbO and to the obtaining of a better crystallized PMN perovskite (PMN1).

Both PMN samples isothermally treated at 870°C are single phase, the perovskite main peaks being more intense for PMN1, which shows a better crystallinity for this compound, obtained by using of the MgO precursor. The temperature increasing at 1200°C determines, beside the enhancing of the perovskite peaks intensity, also the appearance of small amounts of pyrochlore phases, as a result of the PMN decomposition process, which is also reported in [27]. This process is more obvious for PMN2 composition (Figs 5a and b).

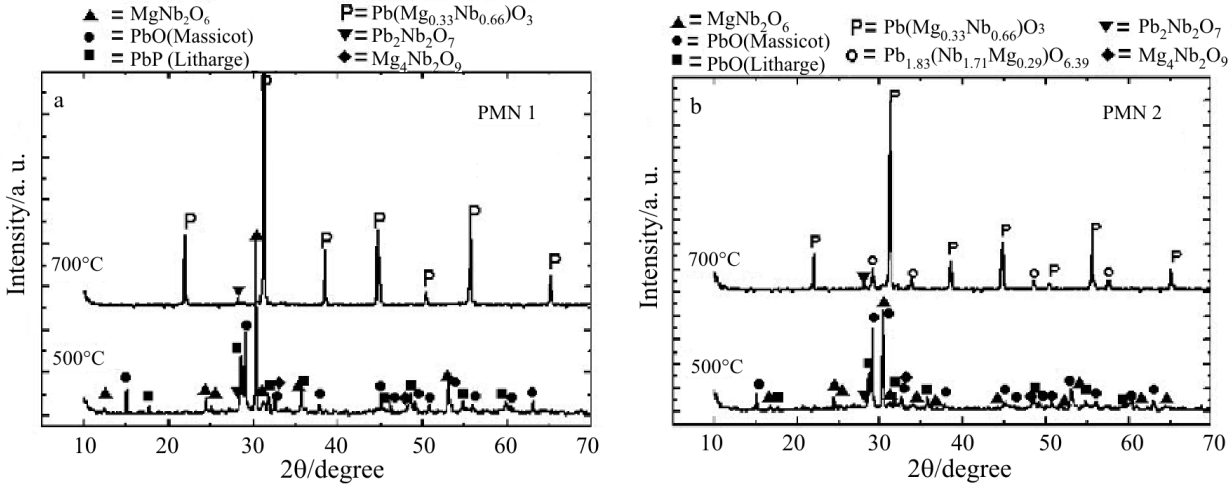

Fig. 4 XRD patterns of PMN samples non-isothermally treated at 500 and 700°C: a – PMN1; b – PMN2

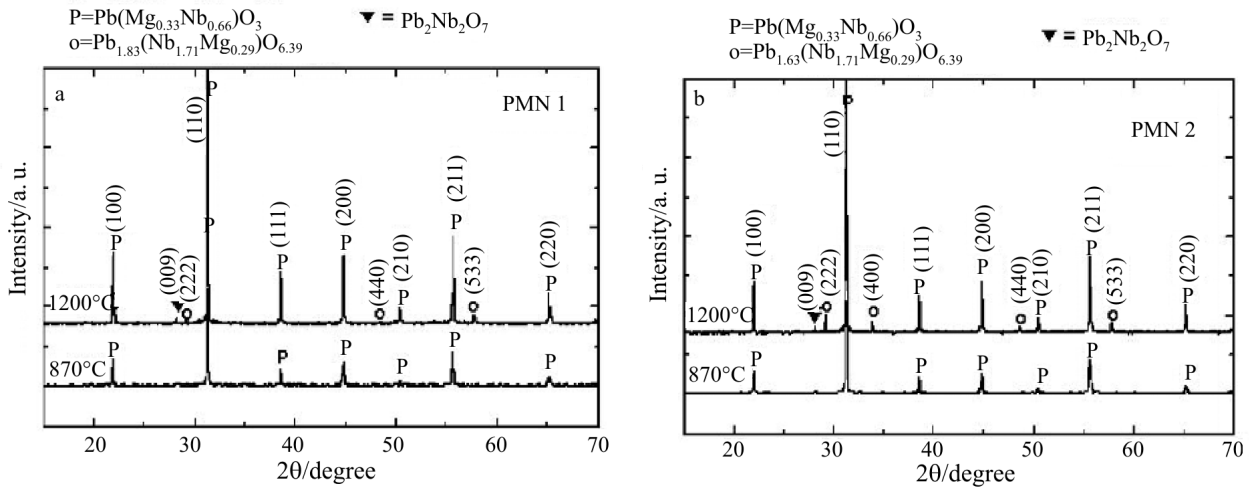

Fig. 5 XRD patterns of the PMN samples isothermally treated at 870 and 1200°C: a – PMN1; b – PMN2

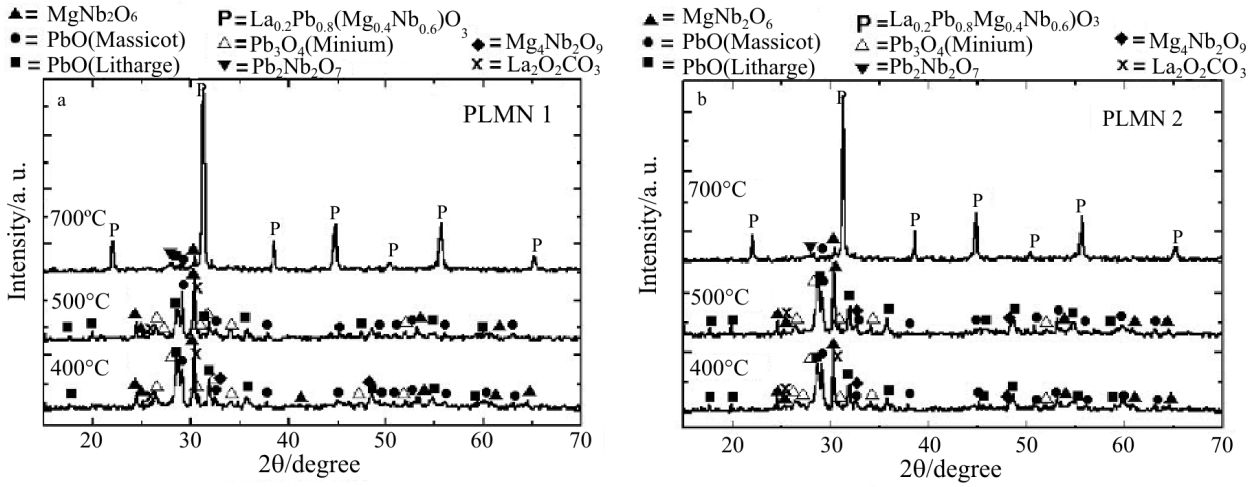

Fig. 6 XRD patterns of the PLMN samples non-isothermally treated at 400, 500 and 700°C: a – PLMN1; b – PLMN2

In the case of the La-modified PMN (PLMN1, PLMN2) mixtures (Figs 6a and b), the X-ray patterns obtained for the powders non-isothermally treated at 400 and 500°C emphasized the presence of the Pb_3O_4 beside the other reactants identified also for PMN1 and PMN2 mixtures, which is in agreement with thermal analysis data. Traces of La precursor ($La_2O_2CO_3$) were also detected. At 700°C, for both PLMN1 and PLMN2 compositions, the perovskite major phase and small amounts of PN pyrochlore and unreacted PbO and $MgNb_2O_6$ were identified. In comparison with the PMN2 sample, in PLMN2 no $Pb_{1.83}(Mg_{0.29}Nb_{1.71})O_{6.39}$ pyrochlore phase was detected.

For isothermally treated PLMN samples, unlike the PMN compositions, the secondary PN pyrochlore phase was detected even at 870°C (Fig. 7).

The temperature rise at 1200°C leads to the increasing of the diffraction peaks belonging to the

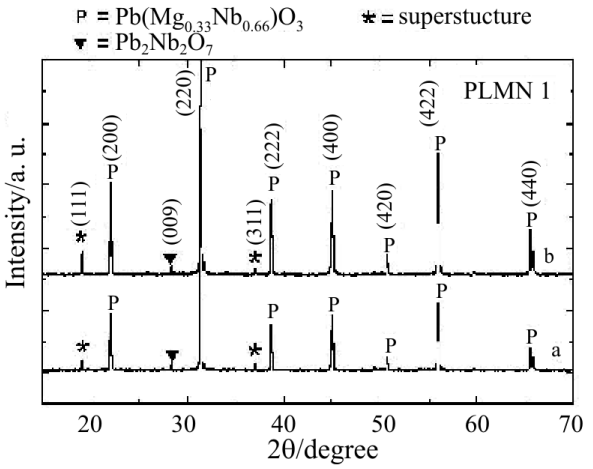

Fig. 7 XRD patterns of PLMN1 sample isothermally treated at: a – 870 and b – 1200°C

Table 2 Lattice parameters for PMN and PLMN compositions isothermally treated at 1200°C/4 h

Sample	Lattice parameter, a/Å	Unit cell volume, V/Å^3	Z	Theoretical density, ρ_t/g cm^{-3}	Apparent density, ρ_a/g cm^{-3}	Relative density, $\rho_r=\rho_a/\rho_t$/%
PMN 1	4.048	66.3318	1	8.145	7.741	95.02
PMN 2	4.047	66.2826	1	8.151	7.727	94.80
PLMN 1	8.050	521.6601	8	7.815	6.653	85.09
PLMN 2	8.045	520.6887	8	7.830	5.803	74.07

perovskite and pyrochlore phases. Besides, one can notice that the La additive induces a short range ordering pointed out by supplementary (111) and (311) diffraction peaks, corresponding to a superstructure formation. These extra peaks can be indexed as {h+1/2, k+1/2, l+1/2} ordered reflections with respect to the fundamental reflections. Although La incorporation into the perovskite lattice determines a unit cell shrinkage because of the smaller ionic radius of La^{3+} compared with Pb^{2+} (1.14 *vs*. 1.20 Å), due to the superstructure formation, the effective lattice parameters of the ordered structures are twice than those of the disordered PMN structures. The values of the lattice parameters, unit cell volume and theoretical density for the compositions considered are presented in Table 2.

Taking into account that the PLMN1 and PLMN2 X-ray diffraction patterns are quite similar we concluded that for the La-modified samples the influence of Mg precursor is less obvious than in the case of pure PMN samples.

Scanning electron microscopy

SEM analyses were performed on the surface of the pellets isothermally treated at 870 and 1200°C.

From the grain size point of view, PMN1 sample annealed at 870°C exhibits a relative homogeneous microstructure consisting of grains with well delimited junctions and an average size of 2.5 μm. Randomly distributed intergranular pores are also noticed (Fig. 8a). The SEM micrograph of the sample annealed at 1200°C shows a heterogeneous microstructure with smaller grains (of ~5 μm) and larger grains (of ~10 μm) as a consequence of the thermally activated grain growth process. One can notice the lack of any inter- or transgranular porosity and perfect triple grain junctions (Fig. 8b). The presence of PbO appearing mostly as white needles in the grain boundaries [28] of the specimen proves the formation during the heating process of a small amount of liquid phase, which seems to crystallize throughout the cooling [5].

The microstructures of PMN2 samples sintered at 870 and 1200°C, respectively, are similar with those corresponding to PMN1 samples sintered at the same temperatures, which indicates no significant effect of Mg precursor on the samples microstructure. This assertion is sustained also by the relative density values, which are very close for the samples consisting of pure lead magnesium niobate, irrespective of the magnesium precursor used for the synthesis (Table 2).

While the SEM micrograph of PLMN1 sample at 870°C is close to that one of PMN1 sample at the same temperature, the image at 1200°C suggests that the lanthanum addition influences dramatically the microstructure only at high temperature (Figs 9a and b). One can observe the inhibitor effect of the lanthanum used as additive on the grain growth process and, consequently, a relative homogenous microstructure, with intergranular porosity, not well-defined grain boundaries and finer grains (of ~3.5 μm) than the similar, non-modified sample.

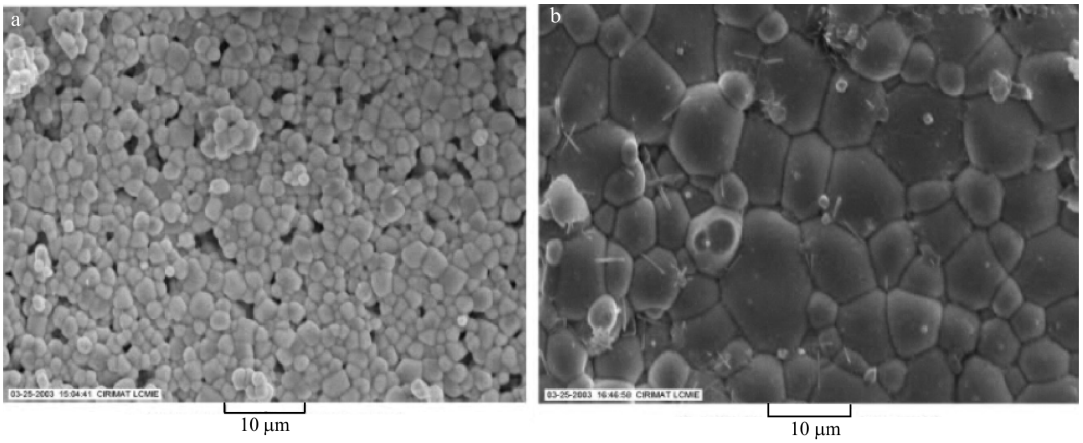

Fig. 8 SEM micrographs of PMN1 sample isothermally treated at: a – 870°C; b – 1200°C

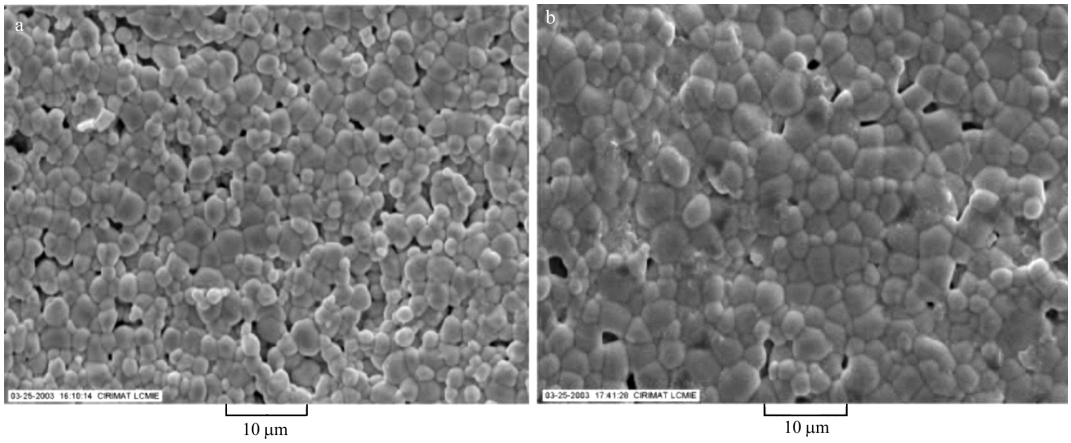

Fig. 9 SEM micrographs of PLMN1 sample isothermally treated at: a – 870°C; b – 1200°C

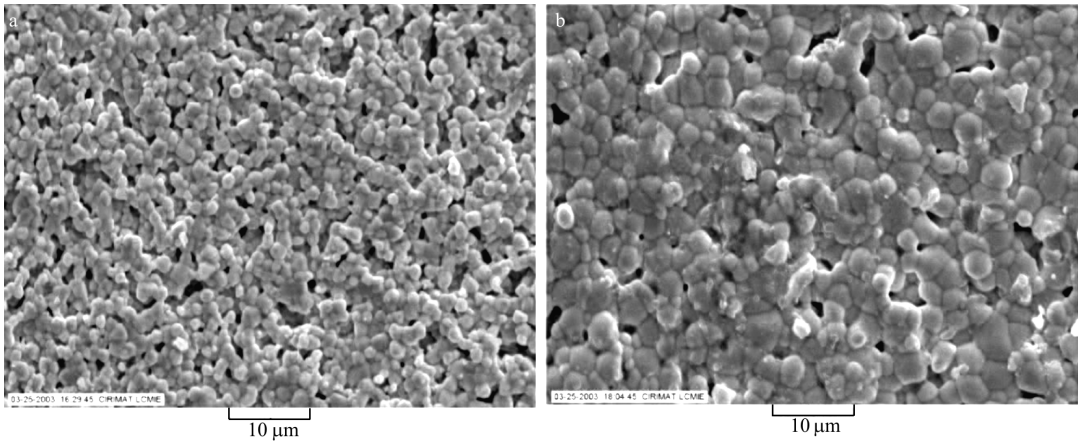

Fig. 10 SEM micrographs of PLMN2 sample isothermally treated at: a – 870°C; b – 1200°C

In the case of PLMN2 specimen the inhibitor effect of lanthanum is also very pregnant at 1200°C, but unlike the PLMN1 sample this effect is visible even at 870°C (the average grain size is about 1.5 μm), suggesting that the incorporation of the additive occurs at lower temperatures when the magnesium carbonate was used as precursor (Figs 10a and b).

Consequently, the intergranular porosity resulted as effect of the fine-grained microstructure induced by the lanthanum admixture affects significantly the densification of PLMN ceramics, which, comparing with pure PMN, shows lower value of relative density, especially when magnesium carbonate was used as precursor.

Conclusions

From the results obtained the following aspects concerning the formation of pure PMN and La-modified PMN using different Mg precursors were pointed out:

- The magnesium precursor type influences the phase composition of the columbite powder resulted in the first stage of PMN synthesis; in order to obtain a pyrochlore free perovskite the amount of $Mg_4Nb_2O_9$ secondary phase in the columbite samples have to be avoided or at least minimized. From this point of view the using of MgO precursor seems to be more favourable for the obtaining of a single phase ceramic comparing to the Mg carbonate precursor.
- By using the columbite route and the mechanical activation for the PMN preparation, a well-crystallized perovskite phase, stable in the temperature range of 800–1200°C was obtained.
- A possible sequence of reactions between PbO and $MgNb_2O_6$ could be written as:

$$PbO+MgNb_2O_6 \xrightarrow{450^\circ C} Pb_3O_4+MgNb_2O_6 \xrightarrow{580^\circ C}$$

$$PbO\ (Massicot+Litharge)+MgNb_2O_6 \rightarrow$$

$$\xrightarrow{680^\circ C} Pb_3MgNb_2O_9(Perovskite)+$$

$$+Pb_2Nb_{2-x}Mg_xO_{7-\delta}(Pyrochlore) \xrightarrow{870^\circ C}$$

$$Pb_3MgNb_2O_9(Perovskite).$$

- For the lanthanum modified PMN samples, the influence of magnesium precursor is less obvious than in the case of pure PMN ceramics, irrespective of the isothermal or non-isothermal annealing; for

both PLMN1 and PLMN2 specimens no pure perovskite phase was obtained.

- The using of the lanthanum-based admixture determines the incorporation of the La^{3+} on Pb^{2+} site; consequently, the presence of La^{3+} cations implies the increase of the short range ordering, as a result of the negative space charge balance into the ordered domains in PMN perovskite structure. The doubling of the unit cell parameter proves the perovskite-like superstructure formation.
- At microstructural level, for the PLMN samples the refinement of the microstructure was pointed out, because of the inhibiting effect of lanthanum on the grain growth process.
- The influence of the magnesium precursor for the PLMN samples is more obvious from microstructural point of view; unlike the PLMN1 sample, for the PLMN2 sample the lanthanum inhibitor effect is visible even at 870°C, suggesting that the incorporation of the additive occurs at lower temperatures when the magnesium carbonate was used as precursor.
- The presence of lanthanum in the perovskite PMN lattice affects the ceramics sinterability estimated by relative density values, significantly lower for PLMN specimens comparing with highly-densified (ρ_r~95%) PMN ceramics.

References

1 T. H. Shrout and A. Halliyal, Am. Ceram. Soc. Bull., 66 (1987) 704.
2 D. H. Kang and K. H. Yoon, Ferroelectrics, 87 (1988) 255.
3 A. L. Costa, C. Galassi, G. Fabri, E. Roncari and C. Capiani, J. Eur. Ceram. Soc., 21 (2001) 1165.
4 S. L. Swartz and T. R. Shrout, Mater. Res. Bull., 17 (1982) 1245.
5 H. C. Wang and W. A. Schulze, J. Am. Ceram. Soc., 73 (1990) 825.
6 J. Chen, A. Gorton, H. N. Chan and M. P. Harmer, J. Am. Ceram. Soc., 69 (1986) C-303.
7 J. Wang, X. Junmin, W. Dongmei and N. Weibeng, Solid State Ionics, 124 (1999) 271.
8 J. Wang, X. Junmin, W. Dongmei and N. Weibeng, J. Am. Ceram. Soc., 82 (1999) 1358.
9 X. Junmin, J. Wang and T. M. Rao, J. Am. Ceram. Soc., 84 (2001) 660.
10 J. Chen, H. M. Chan and M. P. Harmer, J. Am. Ceram. Soc., 72 (1989) 593.
11 Z. Xu, Surya M. Gupta, D. Viehland, Y. Yan and S. J. Pennycook, J. Am. Ceram. Soc., 83 (2000) 181.
12 M. Koyuncu and S. M. Pilgrim, J. Am. Ceram. Soc., 82 (1999) 3075.
13 P. A. Joy and K. Sreedhar, J. Am. Ceram. Soc., 80 (1997) 770.
14 J. Chen and M. P. Harmer, J. Am. Ceram. Soc., 73 (1990) 68.
15 A. Ianculescu, A. Brãileanu, M. Zaharescu, I. Pasuk, E. Chirtop, C. Popescu and E. Segal, J. Therm. Anal. Cal., 64 (2001) 1001.
16 A. Ianculescu, A. Brãileanu, I. Pasuk and M. Zaharescu, J. Therm. Anal. Cal., 66 (2001) 501.
17 A. Ianculescu, A. Brãileanu, M. Zaharescu, S. Guillemet, I. Pasuk, J. Madarász and G. Pokol, J. Therm. Anal. Cal., 72 (2003) 173.
18 A. Brăileanu, A. Ianculescu, M. Zaharescu, I. Pasuk, J. Madarász, G. Pokol and S. Preda, Key Eng. Mater., 264–268 (2004) 309 .
19 L.-J. Lin and T.-B. Wu, J. Am. Ceram. Soc., 73 (1990) 1253.
20 L.-J. Lin and T.-B. Wu, J. Am. Ceram. Soc., 74 (1991) 1360.
21 D. M. Fanning, I. K. Robinson, S. T. Jung, E. V. Colla, D. D. Viehland and D. A. Payne, J. Appl. Phys., 87 (2000) 840.
22 K. Park, L. Salamanca-Riba, M. Wuttig and D. Viehland, J. Mater. Sci., 29 (1994) 1284.
23 X. Pan, W. D. Kaplan, M. Rühle and R. E. Newnham, J. Am. Ceram. Soc., 81 (1998) 597.
24 Differential Thermal Analysis, Edited by R. C. Mackenzie, Academic Press, London and New York 1970, p. 315.
25 K. Sreedhar and A. Mitra, Mater. Res. Bull., 32 (1997) 1643.
26 N.-K. Kim, Mater. Lett., 32 (1997) 127.
27 S. M. Gupta and A. R. Kulkarni, Mater. Chem. Phys., 39 (1994) 98.
28 J. P. Guha, J. Eur. Ceram. Soc., 23 (2003) 133.